An integrated gaseous detector using microfabrication post-processing technology

V.M. Blanco Carballo, C. Salm, S.M. Smits, J. Schmitz, M. Chefdeville, H. van der Graaf, J. Timmermans and J.L. Visschers
University of Twente/MESA+ Institute
Hogekamp 3214 P.O. Box 217, 7500 AE Enschede, the Netherlands
Phone: +31 (0)53 4892 729 Fax: +31 (0)53 4891 034
E-mail: v.m.blancocarballo@utwente.nl

Abstract—**this paper presents the operational characteristics of several integrated Micromegas detectors. These detectors called InGrids are made by means of micro-electronic fabrication techniques. These techniques allow a large variety of detector geometry to be made and studied. Gain, gain homogeneity and energy resolution were measured for various amplification gap sizes, hole pitches and hole diameters in Argon/Isobutane. Gain measurements as a function of gap thickness are compared to the Rose and Korff formula and a model of the detector gain. Our model uses electric field maps and MAGBOLTZ calculated amplification coefficients.**

***Keywords*— Integrated Micromegas; wafer post-processing; gain; energy resolution**

I. INTRODUCTION

Microfabrication techniques have dramatically improved the performance of gaseous detectors. Devices such as Micromegas [1] and GEM [2] make use of these techniques during their fabrication process to achieve high granularity, homogeneity and good spatial resolution. Punctured membranes can be produced with high precision, and hole sizes and pitches can be adapted easily to the specific needs. But despite using high accurate techniques to build the detector itself, the final mounting step over the readout plane is made manually. This inherently comes with several disadvantages, like misalignment between holes and pixels, Moiré effect, dead pixel areas, human errors and problems to reach volume production.

The successful realization of the InGrid detector by Chefdeville et al. [3] is a major step towards the fully integrated gaseous detector. The process is IC compatible so the grid can be integrated directly on a pixel readout chip in a wafer post processing step with good alignment between holes and pixels. The pillar diameter can be shrunk to 30 μm so that the pillars fit in between the grid holes resulting in 100% detection area. Both the pillar height (amplification gap) and the grid design (hole shape, pattern and size) can be accurately controlled. This offers new design space for the detector optimization.

In this work several InGrid prototypes have been made and their operational characteristics measured. The experimental setup and fabrication process were presented in ref. [3]. All measurements have been done using a 80/20 Argon/Isobutane gas mixture. The next section describes our approach to model the detector gain; sections 3, through 6 discuss gain and energy resolution measurements and modelling results.

II. GAIN MODELING

Under the assumption that secondary processes and attachment are negligible, the gas gain in a high electric field is governed by the primary Townsend coefficient α(E), the mean number of ion pairs formed per unit length by an electron at an electric field E. A single electron traversing a path along the z direction will on average cause a total gain G of

$$G = e^{\int \alpha(E(z))\,dz} \quad (1)$$

In the case of a homogeneous electric field, α is constant and the equation simplifies to

$$G = e^{\alpha g} \quad (2)$$

with g the projected track length (the distance between the two plates in a parallel-plate geometry).

The electric field in the Micromegas detector is generally approximated as a composition of a homogeneous low (drift) field region (Ed) and a

homogeneous high field region (Ea). This assumption allows to define the field ratio (Ea/Ed) and to model the collection efficiency and the ion backflow in terms of this field ratio. In this study we found the precise field shape at intermediate field strength (i.e. near the foil openings) to be crucial for the overall detector performance, see sections 3 and 5.

To estimate the gain of a Micromegas detector, the Townsend coefficient then must be integrated along the electron drift path. The statistical variation in electron trajectories and collision phenomena is accounted for by Monte Carlo calculations as provided by the program GARFIELD [4], using the electric field maps from MAXWELL 3D [5] and amplification and drift coefficients from MAGBOLTZ [6].

III. GAIN HOMOGENEITY

The microelectronic fabrication techniques (spin coating, sputtering and wet etching) used to make the InGrids allow an accurate control of the gap thickness, the grid thickness and the hole diameter, resulting in a very good gain homogeneity (defined as the RMS relative variation of gas gain across a prototype).

For several InGrids, the gain was measured on ten equally spaced locations across the active area by means of a collimator. The homogeneity was found to be 10 % in the worst case and 1.6 % in the best one (Figure 1).

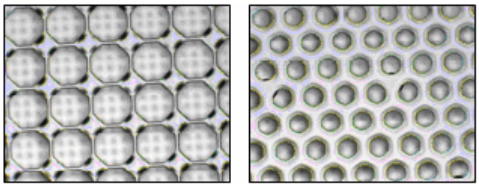

Figure 1: A 80-µm hole pitch, 75-µm gap InGrid, showing 10% gain homogeneity (left side) and a 60-µm hole pitch, 35-µm gap InGrid exhibiting 1.6 % gain homogeneity with a 240 µm pillar pitch (right side)

For a given gap thickness, the gain homogeneity was measured to degrade for larger hole diameters. Inversely, for a given grid geometry, it was improving for smaller gap thicknesses. We believe the gain to be more sensitive to hole diameter and gap thickness variations in the case of bigger holes.

This sensitivity difference was simulated using the method described in section 2. Gains of a large and a small hole configuration of 75-µm gap were calculated. Same operation was done for hole diameters and gap thicknesses differing +/-10% of their original values. Results are summarized in tables 1,2 and show that the large hole configuration is more sensitive to diameter variations while both are almost as sensitive to gap variations.

Hole Ø (µm)	ΔØ/Ø (%)	ΔG/G (%)
36	10	19
	-10	6
70	10	30
	-10	19

Table 1 : Gain sensitivity to hole diameter variations.

Hole Ø (µm)	Δg/g (%)	ΔG/G (%)
36	10	45
	-10	40
70	10	43
	-10	38

Table 2: Gain sensitivity to gap thickness variations

IV. GAIN AND GAP THICKNESS

One particularly interesting feature of the Micromegas detector that can be studied with InGrid is the dependence of the gain with the gap thickness. For a given grid voltage, increasing the gap thickness reduces the field but increases the available amplification length [8]. If equation (1) holds, the gap thickness dependence of the gain will be governed by the field dependence of the Townsend coefficient.

An empiric formula valid for low fields was derived by Rose and Korff [7, 8]:

$$\alpha = APe^{-BP/E} \quad (3)$$

where P is the pressure, E the electric field strength and A and B constants of the gas mixture. Replacing E by V/g (V being the grid voltage) and using (1) leads to:

$$G = e^{gAPe^{-gBP/V}} \quad (4)$$

For a given gas, pressure and grid voltage V, the gain presents a maximum for a certain gap thickness.

$$g(G_{\max}) = V/(BP) \quad (5)$$

Selecting the gap thickness according to equation 5 should make the gain to a certain extent insensitive to mechanical imperfections of the mesh (wrinkles) and of the gap thickness (pillar height variation). This is not a critical point for the InGrid as gap thickness and grid flatness are accurately controlled. It is however interesting to check that there is indeed a gap thickness for which the gain is maximum.

Several devices with gap thicknesses in the range from 35 µm to 75 µm have been built and gain curves have been measured. In figure 2 gain curves as a

function of the grid voltage are shown. The gain curves have been fitted using the Rose and Korff formula.

In figure 3 the dependence of gain with gap thickness is presented. These measurements were performed at almost constant atmospheric pressure (variation less than 2%).

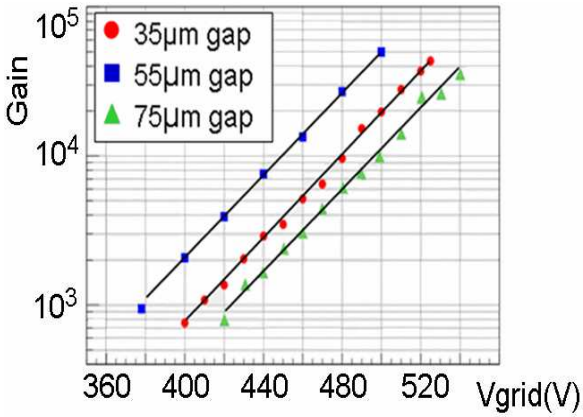

Figure 2: Gain as a function of grid voltage for various gap thicknesses. The data points are fitted using the Rose and Korff formula (lines).

From Figure 3, it is clear that the Rose and Korff formula describes the trend well, even though the fit is not perfect and one requires more measurement points for a critical assessment. The gas gain reaches its maximum value for a gap around 50 µm operated with 450 V on the grid.

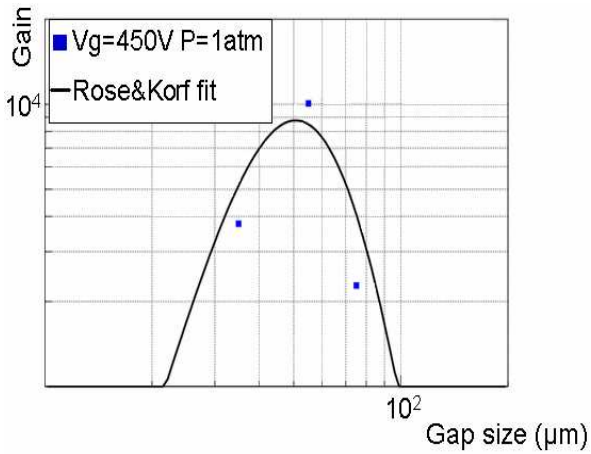

Figure 3: Gain at 450 V on the grid for various gap thicknesses. The data points are fitted using the Rose and Korff formula.

V. GAIN AND GRID GEOMETRY

Gain as a function of grid geometry has been measured for three 75 µm gap InGrids, each of one having a different hole diameter and hole pitch summarized in following Table.

	InGrid 1	InGrid 2	InGrid 3
Hole pitch (µm)	50	60	80
Hole diameter (µm)	32	36	75
Gain @ 500 V	9800	9900	2900

Table 3: Measured gain for different InGrid geometries

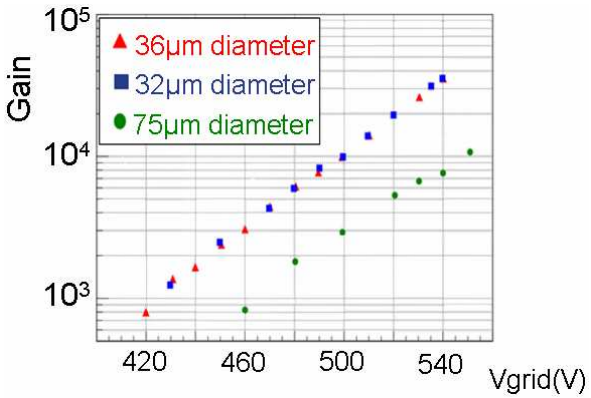

Figure 4: Gain for three grid geometries (see table above).

The gain is clearly dependent on the hole diameter. This is understood by looking at the field strength along the hole axis for different hole diameter, keeping the hole pitch fixed (Figure 5).While decreasing the hole diameter, the electric field along the hole axis is higher over a longer distance, therefore the overall gain increases.

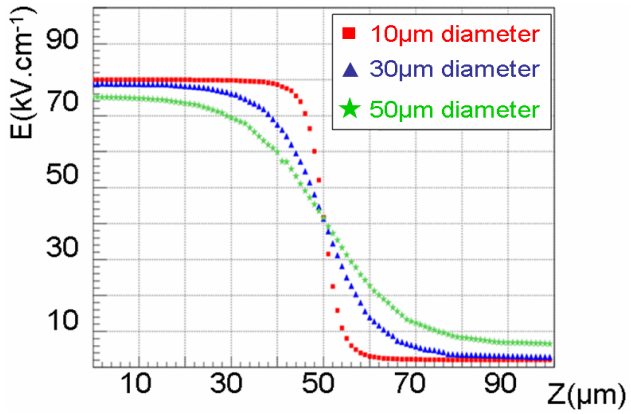

Figure 5: Electric field along the hole axis of a 50-µm gap InGrid for various hole diameters (400 V on the grid).

VI. ENERGY RESOLUTION MEASUREMENTS

The resolution of gaseous detectors is mainly determined by the primary charge fluctuations and the single electron gain fluctuations. These sources are intrinsic to the sensing gas and cannot be avoided. On the other hand, fluctuation sources like attachment and collection efficiency depend on the drift field and can therefore be optimized for minimum energy resolution.

Energy resolution is calculated using 55Fe spectra. 55Fe emits quanta of 5.9 keV and 6.5 keV in the ratio 9 to 1. This ratio is slightly modified to 7.5 to 1, due to the different absorption of these lines in the gas [7]. Spectra were fitted using two Gaussian functions (Figure 6). The parameters (mean, height, width) of the 6.5 keV line were fixed by the ones of the 5.9 keV line. The energy resolution is defined as the FWHM of the 5.9 keV line.

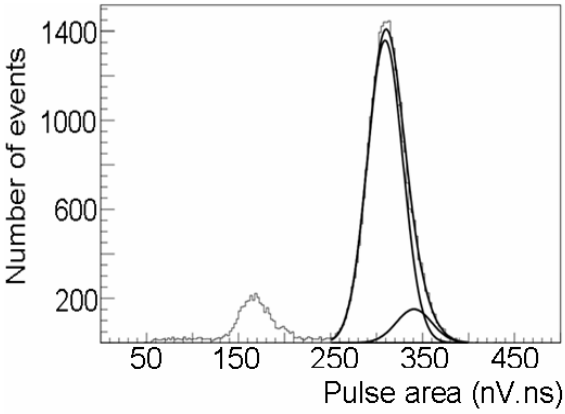

Figure 6: 55Fe spectra in Argon showing the fit of the 5.9 keV and 6.5 keV lines.

For the three grid geometries tabulated in Table 3, the energy resolution was measured as a function of the grid voltage. Remarkably, the three curves almost superimpose when plotted as a function of the gain (Figure 7).

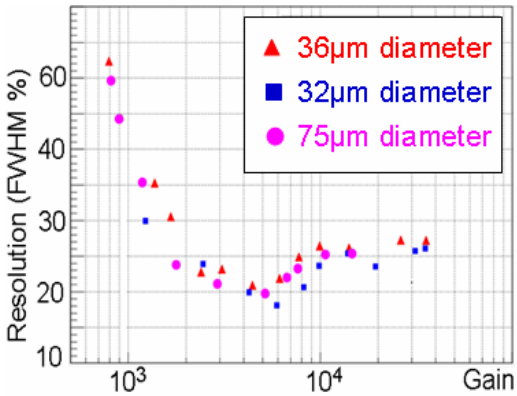

Figure 7: Resolution vs. gain for various hole diameters.

As already noted in [9], the resolution exhibits a minimum with respect to grid voltage (or gain). An explanation of the resolution improvement could be the reduction of avalanche fluctuations when increasing the amplification field i.e. transition from exponential to Polya single electron gain fluctuations. Degradation above a gain of 5.103 could be explained by secondary avalanches induced by UV photons or space charge effects that distort the field.

VII. CONCLUSIONS

The fabrication process of InGrid has reached a mature level and several InGrids of different geometry have been made and tested. Excellent homogeneity of the gas gain across a detector (1.6% RMS) is reported. Gain measurements for different amplification gap thicknesses show a good agreement with the Rose and Korff formula. Energy resolution has been measured to have a minimum at a gain around 5.103 for three 75-µm gap thickness InGrids of different hole pitch and diameter. The obtained results further show that considerable design freedom exists in the hole shape and diameter.

ACKNOWLEDGEMENTS

This research is funded by the Dutch Foundation for Fundamental Research on Matter (FOM) and by the Dutch Technology Foundation STW through project TET 6630 “Plenty of room at the top”. We thank T. Aarnink, D. Altpeter, H. Jansen, J. Melai and A. Boogaard for all their productive discussions.

REFERENCES

[1] Y. Giomataris et al., Nucl. Instr. and Meth. A 376 (1996) 29
[2] F. Sauli, Nucl. Instr. and Meth. A 386 (1997) 531
[3] M. Chefdeville et al., Nucl. Instr. and Meth. A 556 (2006) 490
[4] R. Veenhof, Nucl. Instr. and Meth. A 419 (1998) 726
[5] Ansoft, Maxwell Parameter extractor 3D
[6] S. Biagi, Nucl. Instr. and Meth. A 421 (1999) 234
[7] F. Sauli, CERN yellow report 77-09
[8] Y. Giomataris, Nucl. Instr. and Meth. A 419 (1998) 239
[9] A. Delbart et al., Nucl. Instr. and Meth. A 461 (2001) 84